

Figure 8. a–d. A 73-year-old woman with nonalcoholic steatohepatitis (NASH)-related cirrhosis and tumor thrombus. Contrast-enhanced CT shows increased diameter of the main portal vein caliber with unequivocal enhancing soft tissue within the vein (**a**, *arrow*) and subsequent washout (*arrows*) during portal venous (**b**) and delayed (**c**) phases consistent with tumor thrombus. Coronal image on portal venous phase (**d**) shows the extension of the macrovascular invasion involving the main portal vein (*arrow*) and portal confluence.

Diffusion-weighted images may show restricted diffusion (Fig. 15) in case of macrovascular invasion due to the increased cellularity within the thrombus. Prior studies (32–34) have assessed the potential of restricted diffusion with quantification of apparent diffusion coefficient (ADC) values, obtaining discordant results for the differentiation of portal vein tumor thrombus from bland thrombus. Catalano et al. (33) reported lower ADC values and ADC ratios in tumor thrombi compared to bland portal vein thrombi. In contrast, Sandrasegaran et al. (32) and Ahn et al. (34) did not find any significant differences in ADC values between bland and tumor thrombi. When using the LI-RADS algorithm, restricted diffusion is considered among the additional imaging features suggesting the presence of TIV, but cannot establish the diagnosis without the presence of unequivocal enhancing tumor thrombus. However, DWI may be useful to better delineate the tumor

extension by increasing its conspicuity in case of hypovascular infiltrative HCC (35, 36). Indeed, HCC with macrovascular invasion may be extremely subtle on MRI due to less conspicuous arterial phase hyperenhancement, especially in lesions with infiltrative appearance blending into background cirrhotic parenchyma.

The administration of hepatobiliary contrast agents may be helpful in the identification of an infiltrative parenchymal mass which typically demonstrates hypointensity on hepatobiliary phase (Fig. 16). Gadoxetic acid-enhanced MRI, in particular, has shown excellent sensitivity (81%–93%) and accuracy (92%–95%) in differentiating portal vein tumor thrombus from bland thrombus in a large retrospective study (37).

Other MRI features associated with the presence of macrovascular invasion are a distance less than 2 cm from the lesion, the presence of an HCC larger than 5 cm and por-

tal vein caliber higher than 1.8 cm, due to the mass effect of growing tumor thrombus (32).

PET-CT

Although positron emission tomography-computed tomography (PET-CT) is currently not recommended as primary imaging modality for HCC diagnosis due to its low sensitivity for the detection of smaller or well-differentiated lesions, PET-CT with ^{18}F -fluorodeoxyglucose (^{18}F -FDG) may provide prognostic information for more aggressive and poorly differentiated HCC (3, 38). Moreover, ^{18}F -FDG PET-CT may be required to stage patients with advanced HCC, especially for the detection and evaluation of extrahepatic metastasis (10).

Only a few studies have investigated the potential of PET-CT for the differential diagnosis of bland from tumor thrombus in patients with HCC demonstrating a higher FDG uptake of the tumor thrombus compared with the bland thrombus (39–42). A recent study from Wu et al. (42) reported a sensitivity of 62% and a specificity of 92% for the differential diagnosis of bland from tumor thrombus using ^{18}F -FDG PET-CT, with a mean SUVmax of 4.3 for the tumor thrombus. Moreover, FDG uptake of the tumor thrombus has been demonstrated to be a prognostic factor for overall survival in patients with HCC and macrovascular invasion and may be adopted for risk stratification of these patients (43).

Radiomics

Radiomics is the new frontier of advanced imaging analysis, which is emerging as a promising tool for radiologic diagnosis in several research studies with potential future applications in clinical practice. Radiomics extracts and analyzes quantitative imaging features that reflect the lesion's heterogeneity, providing additional information otherwise undetectable by human eyes. Recently published studies have explored the potential of radiomics and texture analysis in liver imaging for the staging of hepatic fibrosis, differential diagnosis of focal liver lesions, and prediction of survival or treatment response of HCC (44, 45). Regarding portal vein thrombosis, a study performed by Canellas et al. (46) demonstrated an excellent diagnostic performance of CT-based texture analysis for the differentiation of bland from tumor thrombus, which correctly classified 96% of the thrombi. Recently, radiomics has also provided new insights for

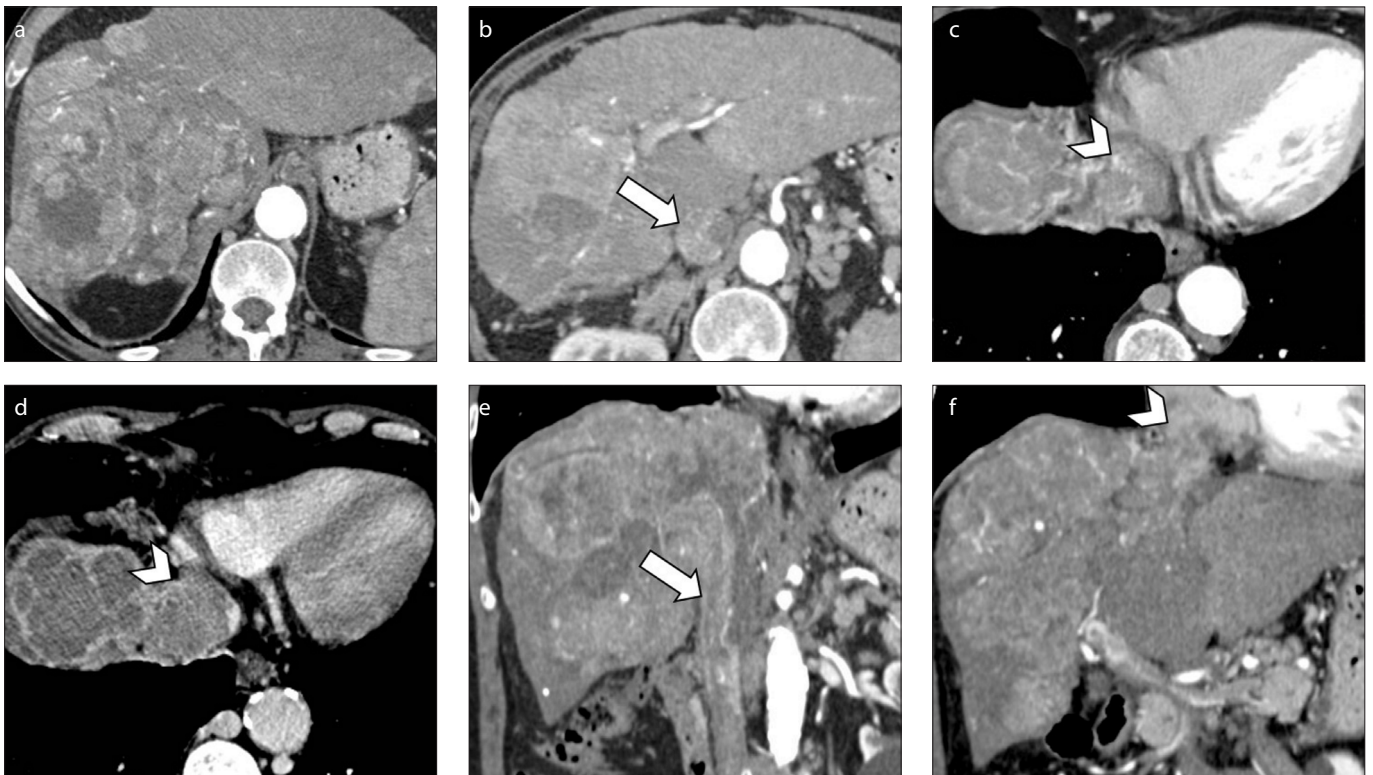


Figure 9. a–f. A 73-year-old man with cirrhosis and HCC with macrovascular invasion. Contrast-enhanced CT image (a) demonstrates a massive HCC involving the whole right hepatic lobe. The HCC is extending into the right hepatic vein along with inferior vena cava (b, *arrow*) and right atrium (c, *arrowhead*). Portal venous phase (d) depicts tumor thrombus involving the vast majority of the right atrium (*arrowhead*). Coronal images (e, f) show the massive macrovascular tumor invasion of the inferior vena cava (*arrow*) and right atrium (*arrowhead*).

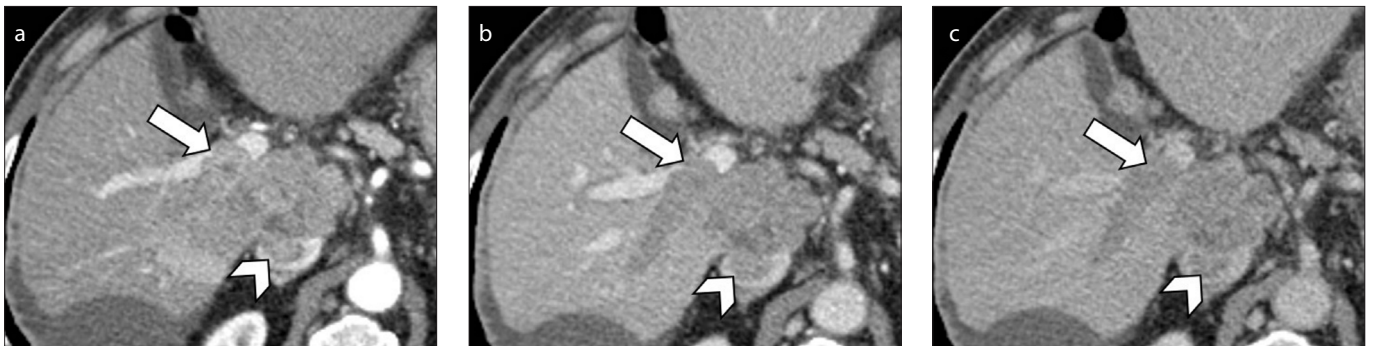


Figure 10. a–c. An 80-year-old man with HBV-related cirrhosis and HCC. Contrast-enhanced CT on hepatic arterial (a), portal venous (b) and delayed (c) phases demonstrate a 4.5 cm HCC in the caudate lobe with macrovascular invasion on both right portal vein branch (*arrows*) and inferior vena cava (*arrowheads*).



Figure 11. a–c. A 75-year-old man with HCV-related cirrhosis, history of treated HCC and co-existence of bland and tumor thrombi. Contrast-enhanced CT on hepatic arterial phase shows enhancing tumor thrombus (a, *arrow*) in the upper branch of the left portal vein and bland non-enhancing thrombus (b, *arrowhead*) in the left portal vein. Coronal images (c) better demonstrate the co-existence of tumor (*arrow*) and bland (*arrowhead*) thrombus in the same patient.

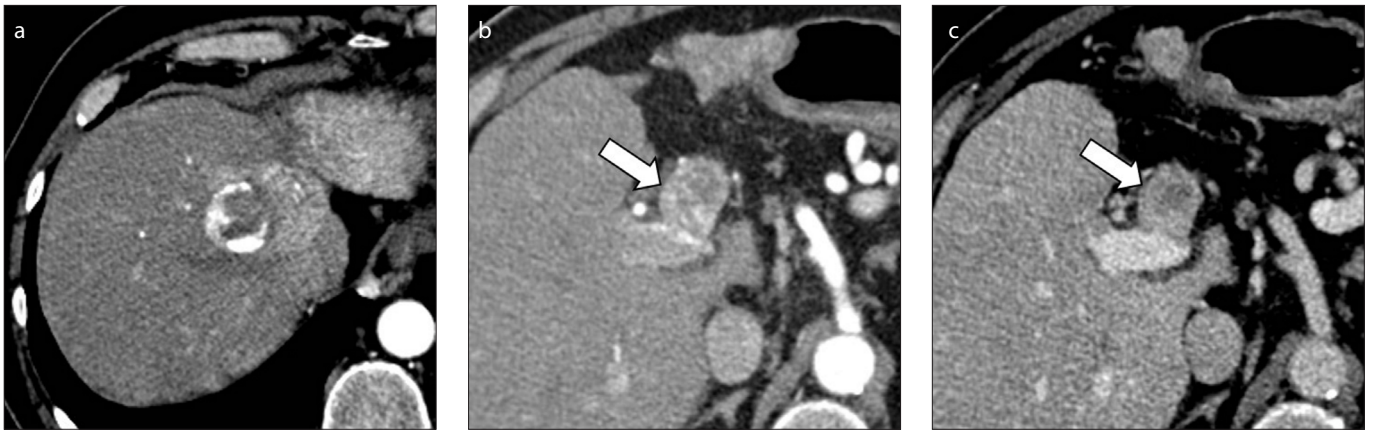


Figure 12. a–c. A 79-year-old man with HCV-related cirrhosis and history of HCC treated with transarterial chemoembolization (TACE). Contrast-enhanced CT on hepatic arterial phase (a) shows treated HCC with TACE with adjacent residual enhancing tumor. CT images on hepatic arterial (b) and portal venous (c) phases at the level of portal vein bifurcation demonstrate macrovascular invasion of the left portal vein (arrows), not present at prior examinations (not shown).

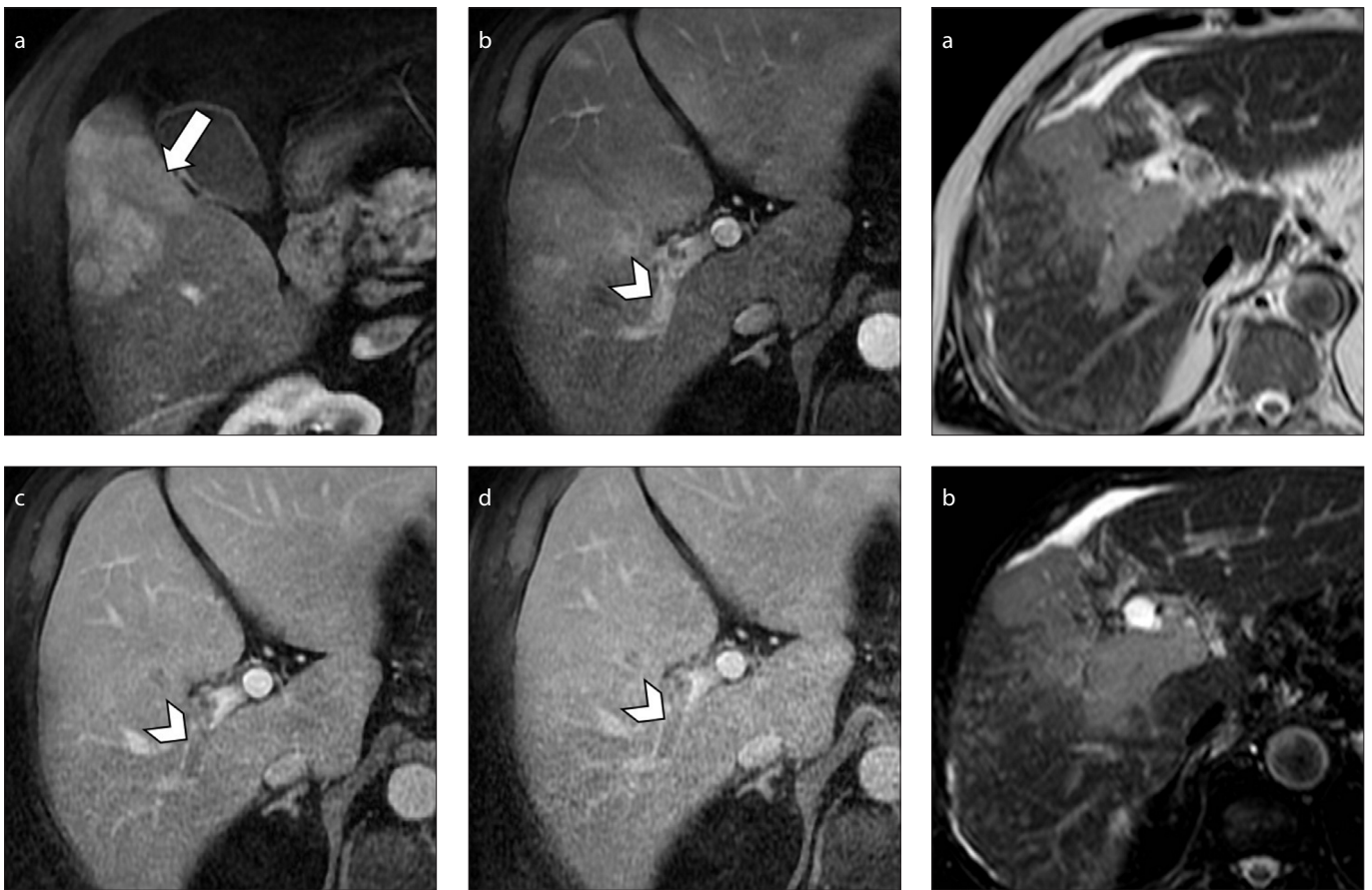


Figure 13. a–d. A 70-year-old man with NASH-related cirrhosis and HCC. MRI on hepatic arterial phase (a) shows a 6.8 cm arterial phase hyperenhancing HCC (arrow). The lesion invades the right portal vein, which demonstrates enhancing tumor thrombus (b, arrowhead) with subsequent washout on portal venous (c) and delayed (d) phases (arrowheads).

Figure 14. a, b. A 71-year-old man with HBV-related cirrhosis and HCC with macrovascular invasion on the right portal vein. The tumor thrombus shows mild-to-moderate hyperintensity on T2-weighted (a) and SPIR images (b).

the noninvasive diagnosis of microvascular invasion in HCC (47, 48), which is one of the few established prognostic factors in HCC. Indeed, unlike macrovascular invasion, microvascular invasion cannot currently be detected at imaging and it is largely diagnosed

postoperatively from pathologic assessment of the tumor specimen.

Treatment

Macrovascular invasion represents an absolute contraindication for locoregional

treatments and significantly limits the therapeutic options. Patients with macrovascular invasion may be candidates for systemic treatment with anti-angiogenic drugs. Particularly sorafenib, a multi-tyrosine kinase inhibitor that suppresses tumor angiogen-

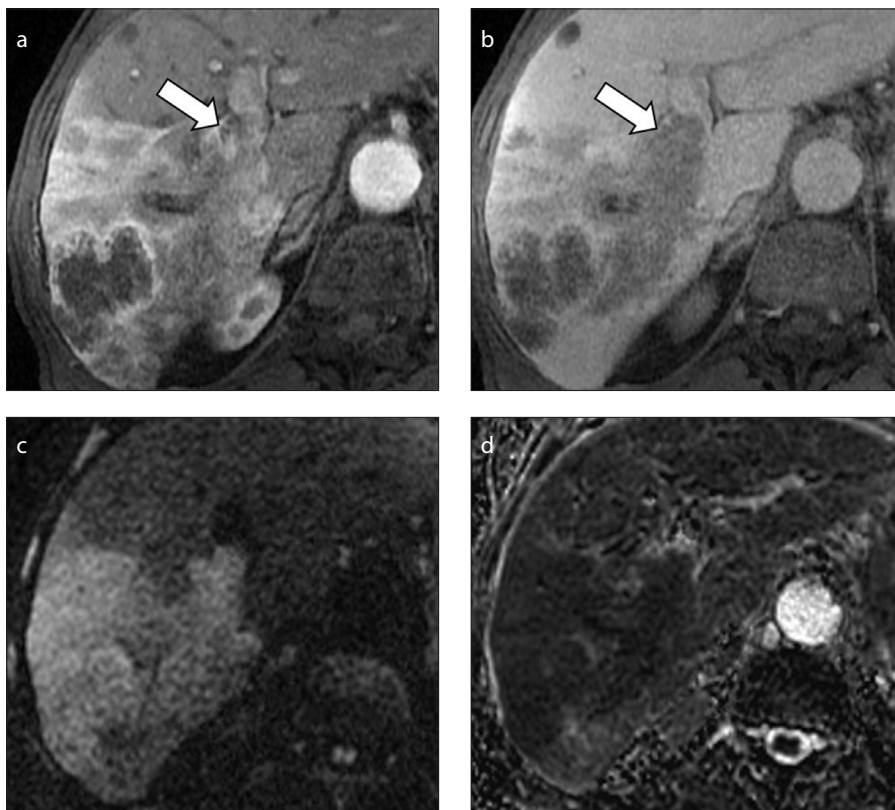


Figure 15. a–d. An 82-year-old man with cirrhosis and history of HCC. MRI images on hepatic arterial (a) and portal venous (b) phases show a large HCC with infiltrative imaging appearance and macrovascular invasion (arrows) in the right portal vein. DWI image at $b = 800 \text{ s/mm}^2$ (c) demonstrates diffusion restriction of the liver mass and hypointensity on ADC map (d).

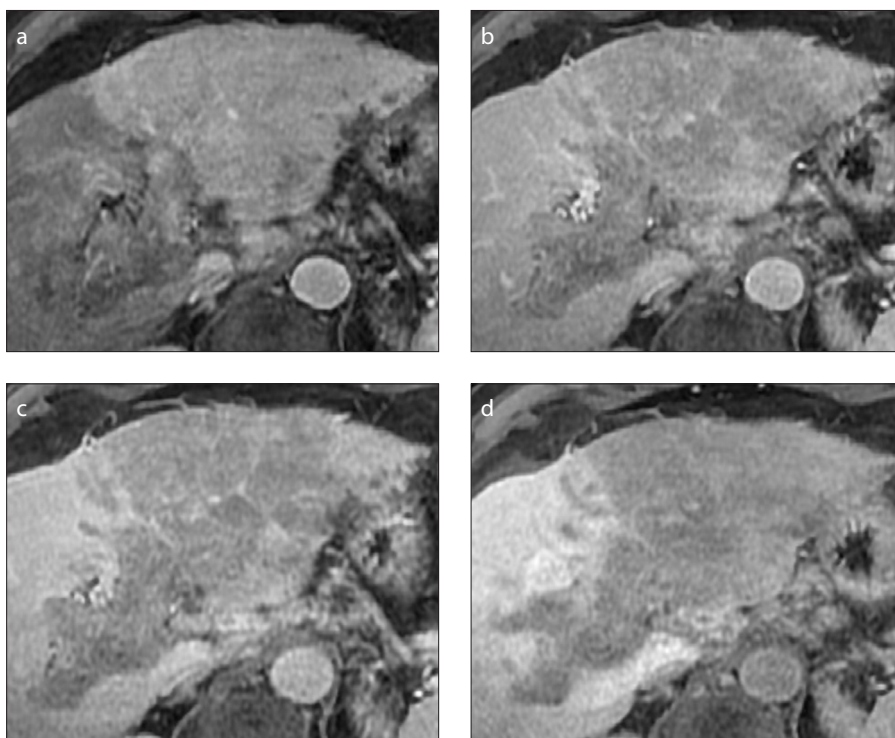


Figure 16. a–d. A 70-year-old woman with cryptogenic cirrhosis and HCC with infiltrative appearance. Gadoteric acid-enhanced MRI shows a large infiltrative HCC with macrovascular invasion of the left portal vein demonstrating mild arterial phase hyperenhancement (a), washout on portal venous phase (b), and hypointensity on 3 minutes transitional (c) and 20 minutes (d) hepatobiliary phases.

esis, has demonstrated to increase the overall survival in patients with advanced stage HCC and it is now considered the standard treatment option in patients with HCC complicated with tumor thrombus (3, 4). As second line therapy, regorafenib, a similar multi-kinase inhibitor, is recommended in patients who progressed after first-line treatment with sorafenib (3).

Conclusion

Macrovascular invasion may be frequently encountered in patients with advanced HCC. Imaging plays a crucial role for the differentiation between bland and tumor thrombi as well as in suggesting the correct underlying etiology. Knowledge of the imaging appearance on diagnostic modalities, each one with their strengths and limitations, may help to improve the diagnostic performance in patients with advanced HCC and guide the clinician towards the most appropriate management.

Conflict of interest disclosure

The authors declared no conflicts of interest.

References

1. Ferlay J, Soerjomataram I, Dikshit R, et al. Cancer incidence and mortality worldwide: sources, methods and major patterns in GLOBOCAN 2012. *Int J Cancer* 2015; 136:E359–386. [Crossref]
2. Llovet JM, Brú C, Bruix J. Prognosis of hepatocellular carcinoma: the BCLC staging classification. *Semin Liver Dis* 1999; 19:329–338. [Crossref]
3. European Association for the Study of the Liver. EASL Clinical Practice Guidelines: Management of hepatocellular carcinoma. *J Hepatol* 2018; 69:182–236.
4. Marrero JA, Kulik LM, Sirlin CB, et al. Diagnosis, staging, and management of hepatocellular carcinoma: 2018 practice guidance by the American Association for the Study of Liver Diseases. *Hepatology* 2018; 68:723–750. [Crossref]
5. Reynolds AR, Furlan A, Fetzer DT, et al. Infiltrative hepatocellular carcinoma: what radiologists need to know. *Radiographics* 2015; 35:371–386. [Crossref]
6. Kneuert PJ, Demirjian A, Firoozmand A, et al. Diffuse infiltrative hepatocellular carcinoma: assessment of presentation, treatment, and outcomes. *Ann Surg Oncol* 2012; 19:2897–2907. [Crossref]
7. American College of Radiology. CT/MRI Liver imaging reporting and data system v2018 Core. <https://www.acr.org/Clinical-Resources/Reporting-and-Data-Systems/LI-RADS/CT-MRI-LI-RADS-v2018>. Accessed on October 2019.
8. Fraum TJ, Tsai R, Rohe E, et al. Differentiation of hepatocellular carcinoma from other hepatic malignancies in patients at risk: diagnostic performance of the Liver Imaging Reporting and Data System Version 2014. *Radiology* 2018; 286:158–172. [Crossref]

9. Park SH, Lee SS, Yu E, et al. Combined hepatocellular-cholangiocarcinoma: Gadoteric acid-enhanced MRI findings correlated with pathologic features and prognosis. *J Magn Reson Imaging* 2017; 46:267–280. [\[Crossref\]](#)
10. Korean Liver Cancer Association; National Cancer Center. 2018 Korean Liver Cancer Association-National Cancer Center Korea Practice Guidelines for the Management of Hepatocellular Carcinoma. *Gut Liver* 2019; 13:227–299. [\[Crossref\]](#)
11. Elsayes KM, Kielar AZ, Chernyak V, et al. LI-RADS: a conceptual and historical review from its beginning to its recent integration into AASLD clinical practice guidance. *J Hepatocel Carcinoma* 2019; 6:49–69. [\[Crossref\]](#)
12. Ludwig DR, Fraum TJ, Cannella R, et al. Hepatocellular carcinoma (HCC) versus non-HCC: accuracy and reliability of Liver Imaging Reporting and Data System v2018. *Abdom Radiol* 2019; 44:2116–2132. [\[Crossref\]](#)
13. Danila M, Sporea I, Popescu A, Şirli R. Portal vein thrombosis in liver cirrhosis - the added value of contrast enhanced ultrasonography. *Med Ultrason* 2016; 18:218–233. [\[Crossref\]](#)
14. Rossi S, Rosa L, Ravetta V, et al. Contrast-enhanced versus conventional and color Doppler sonography for the detection of thrombosis of the portal and hepatic venous systems. *AJR Am J Roentgenol* 2006; 186:763–773. [\[Crossref\]](#)
15. Tarantino L, Francica G, Sordelli I, et al. Diagnosis of benign and malignant portal vein thrombosis in cirrhotic patients with hepatocellular carcinoma: color Doppler US, contrast-enhanced US, and fine-needle biopsy. *Abdom Imaging* 2006; 31:537–544. [\[Crossref\]](#)
16. Raza SA, Jang HJ, Kim TK. Differentiating malignant from benign thrombosis in hepatocellular carcinoma: contrast-enhanced ultrasound. *Abdom Imaging* 2014; 39:153–161. [\[Crossref\]](#)
17. American College of Radiology. Ultrasound LI-RADS® v2017. <https://www.acr.org/Clinical-Resources/Reporting-and-Data-Systems/LI-RADS/Ultrasound-LI-RADS-v2017>. Accessed on October 2019.
18. Bartolotta TV, Taibbi A, Midiri M, Lagalla R. Contrast-enhanced ultrasound of hepatocellular carcinoma: where do we stand? *Ultrasonography* 2019; 38:200–214. [\[Crossref\]](#)
19. Claudon M, Dietrich CF, Choi BI, et al. Guidelines and good clinical practice recommendations for Contrast Enhanced Ultrasound (CEUS) in the liver - update 2012: A WFUMB-EFSUMB initiative in cooperation with representatives of AFSUMB, AIUM, ASUM, FLAUS and ICUS. *Ultrasound Med Biol* 2013; 39:187–210. [\[Crossref\]](#)
20. Rossi S, Ghittoni G, Ravetta V, et al. Contrast-enhanced ultrasonography and spiral computed tomography in the detection and characterization of portal vein thrombosis complicating hepatocellular carcinoma. *Eur Radiol* 2008; 18:1749–1756. [\[Crossref\]](#)
21. Song ZZ, Huang M, Jiang TA, et al. Diagnosis of portal vein thrombosis discontinued with liver tumors in patients with liver cirrhosis and tumors by contrast-enhanced US: a pilot study. *Eur J Radiol* 2010; 75:185–188. [\[Crossref\]](#)
22. American College of Radiology. CEUS LI-RADS® v2017. <https://www.acr.org/-/media/ACR/Files/RADS/LI-RADS/CEUS-LI-RADS-2017-Core.pdf?la=en>. Accessed on October 2019.
23. Dănilă M, Sporea I, Popescu A, Şirli R, Sendroiu M. The value of contrast enhanced ultrasound in the evaluation of the nature of portal vein thrombosis. *Med Ultrason* 2011; 13:102–107. [\[Crossref\]](#)
24. Cannella R, Fowler KJ, Borhani AA, Minervini MI, Heller M, Furlan A. Common pitfalls when using the Liver Imaging Reporting and Data System (LI-RADS): lessons learned from a multi-year experience. *Abdom Radiol* 2019; 44:43–53. [\[Crossref\]](#)
25. Carneiro C, Brito J, Bilreiro C, et al. All about portal vein: a pictorial display to anatomy, variants and physiopathology. *Insights Imaging* 2019; 10:38. [\[Crossref\]](#)
26. Alzubaidi S, Patel I, Saini A, et al. Current concepts in portal vein thrombosis: etiology, clinical presentation and management. *Abdom Radiol* 2019; 44:3453–3462. [\[Crossref\]](#)
27. Sereni CP, Rodgers SK, Kirby CL, Goykhman I. Portal vein thrombus and infiltrative HCC: a pictorial review. *Abdom Radiol* 2017; 42:159–170. [\[Crossref\]](#)
28. Sherman CB, Behr S, Dodge JL, Roberts JP, Yao FY, Mehta N. Distinguishing tumor from bland portal vein thrombus in liver transplant candidates with hepatocellular carcinoma: the A-VE-NA criteria. *Liver Transpl* 2019; 25:207–216. [\[Crossref\]](#)
29. Sorrentino P, Tarantino L, D'Angelo S, et al. Validation of an extension of the international non-invasive criteria for the diagnosis of hepatocellular carcinoma to the characterization of macroscopic portal vein thrombosis. *J Gastroenterol Hepatol* 2011; 26:669–677. [\[Crossref\]](#)
30. Tublin ME, Dodd GD 3rd, Baron RL. Benign and malignant portal vein thrombosis: differentiation by CT characteristics. *AJR Am J Roentgenol* 1997; 168:719–723. [\[Crossref\]](#)
31. Mähringer-Kunz A, Steinle V, Düber C, et al. Extent of portal vein tumour thrombosis in patients with hepatocellular carcinoma: The more, the worse? *Liver Int* 2019; 39:324–331. [\[Crossref\]](#)
32. Sandrasegaran K, Tahir B, Nutakki K, et al. Usefulness of conventional MRI sequences and diffusion-weighted imaging in differentiating malignant from benign portal vein thrombus in cirrhotic patients. *AJR Am J Roentgenol* 2013; 201:1211–1219. [\[Crossref\]](#)
33. Catalano OA, Choy G, Zhu A, Hahn PF, Sahani DV. Differentiation of malignant thrombus from bland thrombus of the portal vein in patients with hepatocellular carcinoma: application of diffusion-weighted MR imaging. *Radiology* 2010; 254:154–162. [\[Crossref\]](#)
34. Ahn JH, Yu JS, Cho ES, Chung JJ, Kim JH, Kim KW. Diffusion-weighted MRI of malignant versus benign portal vein thrombosis. *Korean J Radiol* 2016; 17:533–540. [\[Crossref\]](#)
35. Rosenkrantz AB, Lee L, Matza BW, Kim S. Infiltrative hepatocellular carcinoma: comparison of MRI sequences for lesion conspicuity. *Clin Radiol* 2012; 67:e105–111. [\[Crossref\]](#)
36. Lim S, Kim YK, Park HJ, Lee WJ, Choi D, Park MJ. Infiltrative hepatocellular carcinoma on gadoteric acid-enhanced and diffusion-weighted MRI at 3.0T. *J Magn Reson Imaging* 2014; 39:1238–1245. [\[Crossref\]](#)
37. Kim JH, Lee JM, Yoon JH, et al. Portal vein thrombosis in patients with hepatocellular carcinoma: diagnostic accuracy of gadoteric acid-enhanced MR imaging. *Radiology* 2016; 279:773–783. [\[Crossref\]](#)
38. Park JW, Kim JH, Kim SK, et al. A prospective evaluation of 18F-FDG and 11C-acetate PET/CT for detection of primary and metastatic hepatocellular carcinoma. *J Nucl Med* 2008; 49:1912–1921. [\[Crossref\]](#)
39. Sun L, Guan YS, Pan WM, et al. Highly metabolic thrombus of the portal vein: 18F fluorodeoxyglucose positron emission tomography/computer tomography demonstration and clinical significance in hepatocellular carcinoma. *World J Gastroenterol* 2008; 14:1212–1217. [\[Crossref\]](#)
40. Sharma P1, Kumar R, Jeph S, et al. 18F-FDG PET-CT in the diagnosis of tumor thrombus: can it be differentiated from benign thrombus? *Nucl Med Commun* 2011; 32:782–788. [\[Crossref\]](#)
41. Hu S, Zhang J, Cheng C, Liu Q, Sun G, Zuo C. The role of 18F-FDG PET/CT in differentiating malignant from benign portal vein thrombosis. *Abdom Imaging* 2014; 39:1221–1227. [\[Crossref\]](#)
42. Wu B, Zhang Y, Tan H, Shi H. Value of 18F-FDG PET/CT in the diagnosis of portal vein tumor thrombus in patients with hepatocellular carcinoma. *Abdom Radiol* 2019; 44:2430–2435. [\[Crossref\]](#)
43. Lee JW, Hwang SH, Kim DY, Han KH, Yun M. Prognostic value of FDG uptake of portal vein tumor thrombosis in patients with locally advanced hepatocellular carcinoma. *Clin Nucl Med* 2017; 42:e35–e40. [\[Crossref\]](#)
44. Park HJ, Lee SS, Park B, et al. Radiomics analysis of gadoteric acid-enhanced MRI for staging liver fibrosis. *Radiology* 2019; 290:380–387. [\[Crossref\]](#)
45. Mulé S, Thieffn G, Costentin C, et al. Advanced hepatocellular carcinoma: pretreatment contrast-enhanced CT texture parameters as predictive biomarkers of survival in patients treated with sorafenib. *Radiology* 2018; 288:445–455. [\[Crossref\]](#)
46. Canellas R, Mehrkhani F, Patino M, Kambadakone A, Sahani D. Characterization of portal vein thrombosis (neoplastic versus bland) on CT images using software-based texture analysis and thrombus density (Hounsfield Units). *AJR Am J Roentgenol* 2016; 207:W81–W87. [\[Crossref\]](#)
47. Xu X, Zhang HL, Liu QP, et al. Radiomic analysis of contrast-enhanced CT predicts microvascular invasion and outcome in hepatocellular carcinoma. *J Hepatol* 2019; 70:1133–1144. [\[Crossref\]](#)
48. Ahn SJ, Kim JH, Park SJ, Kim ST, Han JK. Hepatocellular carcinoma: preoperative gadoteric acid-enhanced MR imaging can predict early recurrence after curative resection using image features and texture analysis. *Abdom Radiol* 2019; 44:539–548. [\[Crossref\]](#)